2018-01-1515 Published 13 Jun 2018

Numerical Aeroacoustic Noise Prediction for Complex HVAC Systems

Matthias Tautz University of Erlangen-Nürnberg

Manfred Kaltenbacher Vienna University of Technology

Stefan Becker University of Erlangen-Nürnberg

Citation: Tautz, M., Kaltenbacher, M., and Becker, S., "Numerical Aeroacoustic Noise Prediction for Complex HVAC Systems," SAE Technical Paper 2018-01-1515, 2018, doi:10.4271/2018-01-1515.

Abstract

Reliable tools for the prediction of aeroacoustic noise are of major interest for the car industry and also for the vendors of heating, ventilation and air conditioning (HVAC) systems whose aim is to reduce the negative impact of HVAC noise onto passengers. In this work a hybrid approach based on the acoustic perturbation equations is tested for this purpose. In a first step, the incompressible flow field is computed by means of a commercial finite volume solver. A large eddy simulation turbulence model is used to obtain time resolved flow data, which is required to accurately predict acoustic phenomena. Subsequently, the aeroacoustic sources are computed and conservatively interpolated to a finite element grid, which is used to calculate the sound radiation. This procedure is tested for an HVAC unit, a radial blower and finally for a complete system, which combines these two components. Measurements of the aeroacoustic noise excited by these components are performed in a semi-anechoic chamber. The comparison of spectra obtained from the simulations and the experiments reveals a good agreement up to a specific frequency.

Introduction

The comfort of passengers in cabins of ground vehicles is one major objective in car development. Beside haptics, usability, and smell, the noise environment got into the focus of the car industry in recent years. A low noise level inside the car cabin enables the use of new technologies like hands-free speakerphones and voice control, whose fault liability improves with a lower background noise level. In this context, the noise of the heat, ventilation and air conditioning systems (HVAC systems) plays a significant role.

Typically, vehicle HVAC systems consist of several components which are flown through by the air. The air is sucked in by a radial blower that equips the air with sufficient energy to compensate for the pressure loss of the downstream component. Subsequently, the air passes the HVAC unit, where it is either cooled or heated and distributed into several channels which guide the air to the outlets inside the cabin. Due to the limited installation space and the requirement to regulate the transported air volumes the components of such a system can be very complex with respect to their geometry.

During the design process of HVAC system components the numerical simulation of aeroacoustic noise can be a key step. In contrast to experiments it gives the opportunity to not only measure the acoustic noise but also analyze the flow field and associated structures in the acoustic sources. Furthermore, it gives an insight into the sound propagation field. Hence, it can provide useful information, which designers can utilize to minimize unwanted sound emission.

The aim of this work is to test a hybrid numerical approach for the prediction of aeroacoustic noise on components of HVAC systems. These simulations were carried out in three steps. First of all, an incompressible flow simulation was carried out. Thereby, no acoustic pressure fluctuations are included in the flow results. For this purpose scale resolving turbulence models were used, which provide a detailed insight into the flow structures. Subsequently, aeroacoustic sources were computed on the flow mesh. After their conservative interpolation to a coarser grid the propagation of acoustic waves was computed by means of a finite element solver.

Alternative approaches for the aeroacoustic noise prediction of HVAC systems were proposed by Martínez-Lera et al., who coupled the flow simulation to finite element and boundary element simulations [1]. While latter was easier to use, the former had the advantage to require lower computation time. Another famous approach in this field of application is the lattice Boltzmann method, which enables a direct noise computation and was, for example, used by Aissaoui et al. [2]. Sack et al. [3] recently presented a new approach for flow noise prediction based on the linearized Navier-Stokes equations (LNSE). However, this idea was tested only for geometries of lower complexity than that investigated in this study.

In the following the coupling approach between flow and acoustic simulations will be introduced. Subsequently, its application to an HVAC unit will be outlined. Furthermore, the same approach will be tested on a radial blower of an HVAC system. Finally, the simulation domains of the blower

and the HVAC unit were spliced to yield in simulations which consist of both components.

Hybrid Aeroacoustic Approach

From a physical point of view, the acoustics are a part of the flow field. Thus, if one solves the compressible Navier-Stokes equations one yields flow and also acoustic pressure fluctuations superimposed in one quantity. However, the acoustic pressure fluctuations are of much smaller amplitude than the flow pressure fluctuations and therefore hard to identify from a compressible flow simulation. As a consequence, it is advantageous to use a hybrid approach which separately provides the flow and acoustic fields. The approach used in this work is based on the acoustic perturbation equations (APE) which were derived by Ewert and Schröder [4].

At first the incompressible Navier-Stokes equations (1) and (2) are solved. Thereby, $\boldsymbol{v_i}$ denotes the flow velocity, p denotes the pressure. ρ_0 is the density and ν the kinematic viscosity which are constant fluid parameters.

$$\frac{\partial \boldsymbol{v}_i}{\partial \boldsymbol{x}_i} = 0 \tag{1}$$

$$\frac{\partial \boldsymbol{v}_i}{\partial t} + \rho_0 \frac{\partial \boldsymbol{v}_i \boldsymbol{v}_j}{\partial \boldsymbol{x}_j} = -\frac{\partial p}{\partial \boldsymbol{x}_i} + \rho_0 \nu \frac{\partial^2 \boldsymbol{v}_i}{\partial \boldsymbol{x}_j^2} \tag{2}$$

The obtained flow field does not contain any information about the acoustics due to the missing compressibility of the fluid. The advantage of such a flow simulation is the reduced computational cost in comparison to a compressible simulation.

In order to compute the acoustic propagation a second set of equations, which are also based on the compressible Navier-Stokes equations needs to be solved. The idea of the APE is to split the flow field variables (pressure, velocity and density) into a mean part, a fluctuation part due to the flow, and a fluctuation part due to the acoustics [4]. This approach is similar to the linearized Euler equations (LEE). This splitting technique is based on the assumption, that the acoustic variables are fluctuating and that a compressible medium is required to model acoustic effects. Furthermore, the acoustic scalar potential ψ^a, which allows for the computation of the acoustic particle velocity $\boldsymbol{v}_i^a$ by equation (3) is introduced.

$$\boldsymbol{v}_i^a = -\frac{\partial \psi^a}{\partial \boldsymbol{x}_i} \tag{3}$$

Using these definitions and assumptions, the perturbed convective wave equation (PCWE) (4) can be derived, which makes use of the total differential as defined in equation (5) [5].

$$\frac{1}{c_0^2}\frac{D^2\psi^a}{Dt^2} - \frac{\partial^2 \psi^a}{\partial \boldsymbol{x}_i} = -\frac{b_s}{c_0^2}\frac{Dp}{Dt} \tag{4}$$

$$\frac{D}{Dt} = \frac{\partial}{\partial t} + \left(\overline{\boldsymbol{v}_i} - \overline{\boldsymbol{v}_i^r}\right)\frac{\partial}{\partial \boldsymbol{x}_i} \tag{5}$$

The overlined quantities indicate temporal mean values. The variable $\boldsymbol{v}_i^r$ denotes the rotational velocity, which only needs to be applied in domains which are rotated and c_0 denotes the speed of sound. The flow field and also the acoustic source on the right hand side of equation (4) were computed on the finite volume mesh used during the flow simulation. The factor b_s is a spatial damping factor, which was used to suppress the acoustic sources of coarse mesh cells and to damp the sources in upstream and downstream directions [6]. After a conservative interpolation of the sources to a finite element grid, this mesh is used to compute the acoustic source propagation.

This aeroacoustic approach enables the computation of acoustic sources from incompressible flow data and the sound propagation under consideration of diffraction effects due to the mean flow velocities. The partial differential equation, which has to be solved solely contains the unknown ψ^a. After solving this equation the acoustic pressure p^a can be computed by equation (6).

$$p^a = \rho_0 \frac{D\psi^a}{Dt} \tag{6}$$

Application to HVAC Components

In the following, the simulation of an HVAC unit will be the first example to be shown. This component is typically the most complex part in the whole HVAC system. Subsequently, the simulation of a radial blower will be presented, which is used in many HVAC systems for the air supply. Finally, a simulation will be presented which combines both of these components. The given results have partly previously been presented in [6] and the results of comparable simulations were released in [7].

HVAC Unit

In Figure 1 the HVAC unit is shown as it was set-up during the experiments. These were performed at a semi-anechoic chamber at the University of Erlangen-Nürnberg, thus free field conditions were realized.

FIGURE 1 HVAC unit inside the semi-anechoic chamber surrounded by microphones

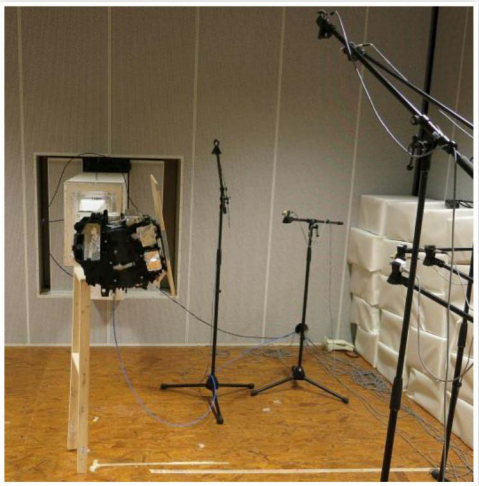

Downstream to the unit a settling chamber was placed to obtain an uniform inflow of a constant mass flow rate of 3.5 kg/min at the intake of the HVAC unit. The heat exchanger of the cooling unit were removed and the inner flaps of the HVAC unit were set up to bypass the heater. Hence, no porous media were needed to be modeled in the simulation. A distribution chamber was also part of the HVAC unit. It contained the intake to several channels, which usually distribute the air to all air outlets in the vehicles cabin. Only one of these outlets was remained open, while the others were closed. By blowing smoke through the HVAC unit remaining leakage openings were detected and closed. Overall seven microphones were placed 1 m away from the remaining open outlet, which were used to validate the acoustic simulation results.

Flow Simulation In order to perform the flow simulations the commercial finite volume solver Star-CCM+ was utilized [8]. This tool was also used to create the flow mesh. Therefore the Trimmed Mesher [8] algorithm was applied, which creates meshes which dominantly consist of hexahedron cells. The finest cell size of 0.3 mm was selected directly at the outlet of the HVAC unit, where the highest flow velocities were expected due to the small cross section area. Downstream to the outlet the mesh was gradually coarsened with the distance to the HVAC unit in the region were a free jet was expected to develop. Inside the HVAC unit a cell size of 1.2 mm was set up. The geometry inside the HVAC unit is rather complex. As a consequence, the creation of many prism layers at the wall could easily yield in a very high cell count and also increases likelihood to obtain cells of bad quality. As a consequence, four layers of prism cells were built up at surfaces, where high flow velocities were expected and the flow was expected to be attached to the wall. At regions which appear as cavities and are bypassed by the main flow only one layer of prism cells was applied. With these prism layer settings a dimensionless wall distance y^+ of about 1 could not be achieved and a wall model was consequently applied. The final mesh consisted of about 40 million cells.

The settling chamber was also modeled by the simulation and a mass flow inlet with a flow rate of 3.5 kg/min was set-up at its inlet. A zero pressure outlet boundary condition was used about 3 m far from the outlet of the HVAC unit. The WALE large eddy simulation turbulence model was selected to model the turbulent scales, which could not be captured by the chosen cell sizes [9]. For the gradient computation the Green-Gauss scheme with a MinMod limiter was chosen and a bounded central difference scheme for the discretization of the convective terms [8]. For the time discretization an implicit second order backward scheme was used with a time step size of $5 \cdot 10^{-6}$s, which was small enough to yield CFL numbers below one. The coupling of flow pressure and flow velocity was realized by the SIMPLE solver algorithm. The source term of the PCWE approach requires the incompressible flow pressure of the flow simulation as input variable. Hence, it is important that the pressure field does not suffer from significant noise, which might be caused by the numerical solving procedure. For this simulation it found to be advantageous to set up a W-Cycling strategy with one pre- and one post-sweep per iteration for the pressure solver to inhibit numerical oscillations [7].

FIGURE 2 Computed velocity magnitude field at one time step inside the HVAC unit

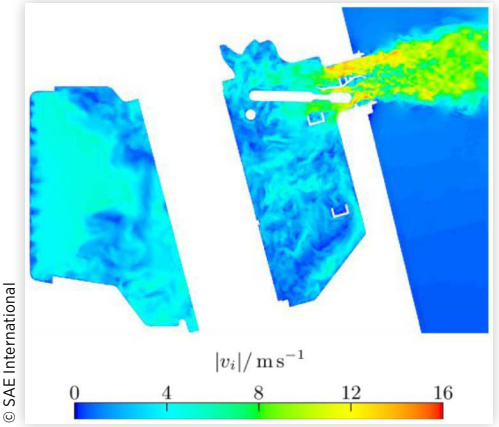

The velocity magnitude field at one time step inside the HVAC unit is depicted in Figure 2. The highest velocities of about 16 m/s occurred directly at the outlet of the unit, where the smallest cells of 0.5 mm edge length were placed. Inside the unit the flow field appeared to be very chaotic and did not seem to have a distinct direction. The pressure loss obtained from the simulation was 107.4 Pa which underestimated the pressure of 121.4 Pa detected during the experiments by about 12%. This could be caused by the low number of prism layers during the simulation. The flow data of about 0.14 s real time was exported for the computation of aeroacoustic sources and the sound propagation simulation.

Acoustic Simulation Prior to the calculation of the sound radiation, the acoustic sources were evaluated on the flow mesh by use of the in-house tool cplreader. The most intense source at the HVAC unit appeared at the outlet close to the throttle flap. Furthermore, sources appeared in the downstream jet. This source region is shown in Figure 3.

In equation (4) the spatial damping function b_s was introduced to spatially blend out the acoustic impact of unwanted sources. This function is one in regions where sources were

FIGURE 3 Computed aeroacoustic source field at one time step at the HVAC unit

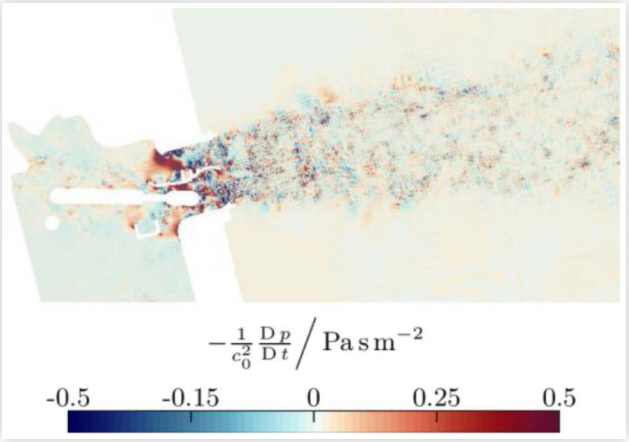

FIGURE 4 Spatial source damping functions for the HVAC unit

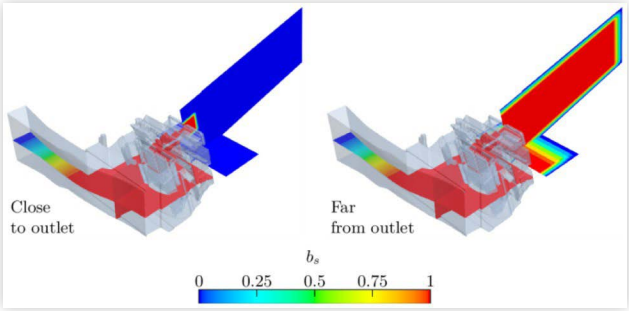

fully recognized and zero were acoustic sources were completely suppressed. In the case of the HVAC unit, two variants of b_s were defined as illustrated in Figure 4. One variant cut the sources very close to the outlet of the HVAC unit. Thus, it did not consider sources of a large part of the jet region. This variant is shown on the left. In contrast the variant of b_s shown on the right side included major parts of the jet.

The acoustic simulation grid was created by use of the meshing tool Ansys ICEM-CFD [8]. In contrast to the flow mesh, it may not contain any polyhedral cells. Two meshing strategies were combined for this case. Inside the HVAC unit itself a unstructured mesh of tetrahedrons was created with an element size of 0.8 mm to 8 mm. At the intake of the HVAC unit and in the far-field a structured mesh of hexahedron cells was created with an element size of 16 mm. Furthermore, three element layers were extruded at the far-field and the inlet, in which a perfectly matched layer (PML) technique was applied to realize free-field boundary conditions for the sound propagation and inhibits reflections of sound waves [11]. Overall the mesh contained about 1.5 million nodes and 3.7 million elements. For the acoustic propagation simulation a coarser time step of 10^{-5}s was chosen. The acoustic propagation simulation was performed by use of the finite element solver CFS++ [12].

The power spectral density (PSD) obtained from these simulation at one far-field microphone position is plotted in Figure 5 against the frequency. At all other far-field microphones the same observations were made.

A good agreement to the experimental results was achieved for frequencies up to about 5 kHz if the damping function was used that cuts the sources close to the outlet. If the damping function far to the outlet was chosen, the numerical noise got dominant for frequencies larger than about 2.5 kHz. This effect could be associated to the cell sizes of the flow mesh. Downstream to the outlet the mesh was gradually coarsened inside the jet region. The damping function far from the outlet features also sources of cells with a size of 4.8 mm whereas the coarsest cells captured by the close damping function are about 0.6 mm large. The coarse cells were not capable to appropriately capture the high frequency components. The pressure signals obtained from these cells of the flow simulation suffered from aliasing effects, which masked the sound signals obtained from the fine mesh placed directly at the outlet.

FIGURE 5 PSD spectra obtained 1 m away from the HVAC unit

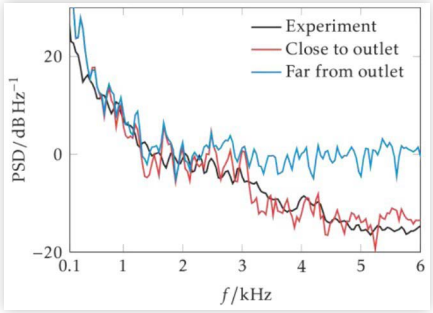

Radial Blower

The chosen radial blower is typically placed into the whole climate system downstream to the HVAC unit. In order to obtain validation results experiments were also performed in a semi-anechoic chamber in a similar way as for the HVAC unit. This measurement set-up is shown in Figure 6.

Far-field microphones were placed about 1 m away from a diffusor, which was placed downstream to the radial housing of the blower itself. The mass flow was set to the same rate as for the HVAC unit to 3.5 kg/min and the rotation rate of the impeller was set to 1860 rpm.

Flow Simulation The solver settings for the flow simulation were selected the same as for the simulation of the HVAC unit. However, a time step size of 10^{-5}s was selected. The flow simulation domain also was required to be split into a stationary domain and a rotating domain which was placed around the impeller blades. Next to the impeller and at the interfaces, which connect these two domains, a cell size of 0.38 mm was selected. Inside the radial housing the cell size set to 0.77 mm. Inside the diffuser and the jet evolving downstream a cell size of 1.54 mm was chosen. Furthermore, four prism cell layers were attached to the wall boundaries. These settings yielded a mesh of 26 million cells, of which about 10 million cells were contained in the rotating region at the impeller.

FIGURE 6 Radial blower inside the semi-anechoic chamber surrounded by microphones

FIGURE 7 Computed velocity magnitude field at one time step inside the radial blower

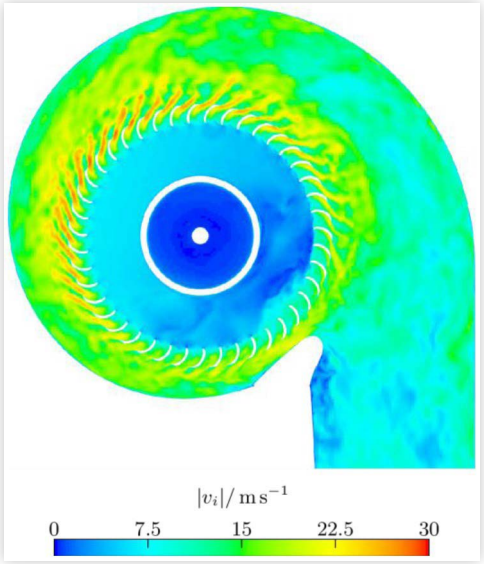

The obtained flow field at one time step inside the radial housing is shown in Figure 7. The maxima of the velocity magnitude are larger than for the HVAC unit and velocities of up to 30 m/s were achieved at the passages between the impeller blades. Downstream the velocities decreased. At the inlet of the simulation domain a pressure of −181.47 Pa was detected during the simulation, which underestimated the pressure of the experiments of −169 Pa by about 7.4%. Hence, the pressure jump due to the blower was accurately reproduced by the flow simulation.

Acoustic Simulation The acoustic sources inside the radial housing are depicted for one time step in Figure 8. The regions of the highest source intensities were between the impeller blades at the angle position, where also the highest

FIGURE 8 Computed aeroacoustic source field at one time step inside the radial blower

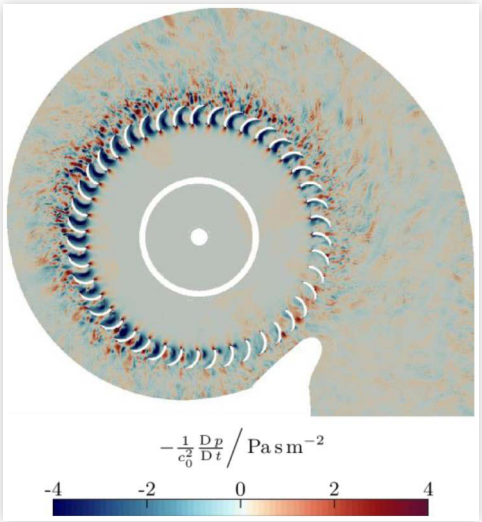

FIGURE 9 Spatial source damping functions for radial blower

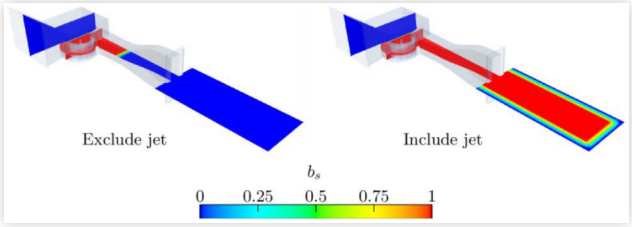

flow velocities were observed. Furthermore downstream to the impeller blades sources appeared. Their intensity rapidly decayed when moving downstream and into the diffuser.

Beside the sources inside the radial housing sources were also noticed in the jet, which formed out downstream to the diffuser as the air leaved the inner channels. According to these source regions two spatial damping functions b_s were defined whose spatial distribution is shown in Figure 9. The function on the right side included the source contributions of the jet whereas this was not done by the function on the left.

For the creation of the finite element grid the same procedure as for the HVAC unit was chosen. An unstructured grid region was created inside the radial housing with an element size of 0.8 to 2 mm at the impeller blades and at the interface. The extent of the rotating domain was chosen to exactly be the same as for the flow simulation. The interface was realized by use if Nitsche's method, which enables the propagation of sound waves across the non-conforming interface. Inside the radial housing an element size of up to 12 mm was chosen. In the far-field and at the inlet structured meshes of hexahedrons with a size of 14 mm were utilized. This mesh contained 0.9 million nodes and 2 million elements.

A PSD spectrum evaluated at one far-field microphone position is shown in Figure 10. In this simulation case no significant differences occurred due to the chosen spatial damping of the source. The jet is actually of minor importance for the acoustics of this blower at the given state of operation. Slight differences appeared at frequencies higher than 3.5 kHz. These could also be associated to the coarsened flow mesh cells inside the jet. Up to about 3.5 kHz both simulations were in excellent agreement with the measurement. The blower had a blade passing frequency of 1.33 kHz at this operating point, which did not occur as a tonal peak in the experiment as well as in the simulation.

FIGURE 10 PSD spectra obtained 1 m away from radial blower

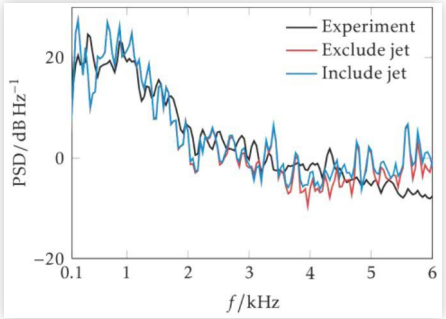

Simulation of the Complete System

After a good agreement with the experimental results could be achieved for the acoustic noise propagation in the far-field for the HVAC unit and also the radial blower, a combined simulation of the complete system was performed. The resulting flow field at one time step of this simulation is depicted in Figure 11. The housing of the components is transparently shown. The simulation domain of the radial blower was spliced to the intake of the HVAC unit downstream to the diffusor. The flow solver settings were chosen equally to the simulation of the radial blower. The smallest cell sizes of 0.375 mm were set up at the impeller and the outlet of the HVAC unit. Also up to four prism cell layers were applied, which yielded in an overall cell size of 54 million cells. Twelve million of these were placed in the rotating region. In the experiments an inlet pressure of −70 Pa was detected, whereas it was −86 Pa in the simulations. This is an underestimation of about 16 Pa. Approximately 10 Pa of these could be associated to the HVAC unit itself and the remaining 6 Pa to the radial blower. Hence, the flow simulation of the complete system obtained pressure fields which were comparable to the pressure fields of the separated components.

The most intense aeroacoustic sources appeared in the same regions that were identified in the previous simulations. These are the outlet of the HVAC unit and at the impeller blades. The chosen spatial damping function was a combination of the damping functions of the radial blower towards the intake side of the system and the damping function close to the outlet of the HVAC unit at the downstream side. For the creation of the acoustic finite element grid the unstructured mesh parts of both components were spliced. The grid at the inlet was taken from the radial blower simulation and the far-field grid with its PML from the HVAC unit simulation. This grid consisted of about 1.8 million nodes and 5.9 million elements. A PSD spectrum in comparison to the experiments is shown in Figure 12. An excellent agreement to the experiments could be achieved for frequencies up to 3.5 kHz. This far-field microphone had the same position relative to the HVAC unit as the microphone chosen for Figure 5. These spectra actually look very similar. This indicates that the

FIGURE 11 Computed velocity magnitude field at one time step inside the complete system

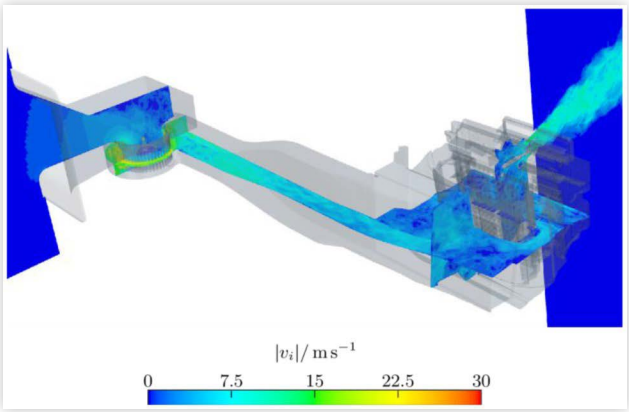

FIGURE 12 PSD spectra obtained 1 m away complete system

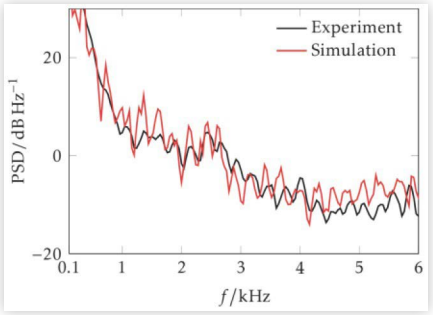

downstream HVAC unit is the major impact factor for the aeroacoustic noise in this complete system. The aeroacoustic noise of the radial blower appeared to be masked. However, it has to noted that the channel, which connects the blower and the HVAC unit, is very long in this configuration, which is typically not the case for these components inside a vehicle where the installation space is limited. If these components would be closer to each other the interaction of their flow and also acoustic fields might increase.

Summary/Conclusions

A simulation procedure was presented, which combined a finite volume flow solver with a finite element acoustic solver. The PCWE were applied to evaluate the aeroacoustic noise propagation.

For the simulation of the HVAC unit a strong dependence of the simulation spectra on the extent of the chosen source domain was observed. Numerical noise of coarse flow mesh cells could have a significant negative effect on the resultant PSD spectra. However, this effect could not be found for the separate simulation of the radial blower. In contrast, no differences occurred during the simulation of the radial blower for different source damping functions. The flow noise propagating from the jet at the diffuser was found to be negligible.

Excellent agreement of the acoustic far-field spectra of simulations and experiments could be achieved for all tested components and configurations. Hence, the given simulation approach was shown to be applicable to HVAC components the prediction of their noise excited by aeroacoustics.

References

1. Martínez-Lera, P., Hallez, R., Beriot, H., and Schram, C., "Computation of Sound in a Simplified HVAC Duct Based on Aerodynamic Pressure," in *18th AIAA/CEAS Aeroacoustics Conference (33rd AIAA Aeroacoustics Conference)*, 2012.
2. Aissaoui, A., Tupake, R.S., Bijwe, V., Meskine, M. et al., "Flow-Induced Noise Optimization of SUV HVAC System Using a Lattice Boltzmann Method," *SAE Int. J. Passeng. Cars - Mech. Syst.* 8(3):1053-1062, 2015, doi:10.4271/2015-01-2323.

3. Sack, S., Shur, M., Åbom, M., Strelets, M. et al., "Numerical Education of Active Multi-Port Data for In-Duct Obstructions," *Journal of Sound and Vibration* 411(22):328-345, 2017.
4. Ewert, R. and Schröder, W., "Acoustic Perturbation Equations Based on Flow Decomposition via Source Filtering," *Journal of Computational Physics* 188(2):365-398, 2003.
5. Kaltenbacher, M., Hüppe, A., Reppenhagen, A., and Kühnel, W., "Coupled CFD-CAA Approach for Rotating Systems," in *Coupled Problems in Science and Engineering VI*, Venice, 2015.
6. Tautz, M., Hüppe, A., Besserer, K., Kaltenbacher, M. et al., "Aeroacoustic Simulation of Complex HVAC Components," in *ICTCA 2017 Vienna - Book of Abstracts*, July 30-Aug. 3, 2017, ISBN:978-3-200-05210-9.
7. Kaltenbacher, M., Hüppe, A., Reppenhagen, A., Tautz, M. et al., "Computational Aeroacoustics for HVAC Systems Utilizing a Hybrid Approach," *SAE Int. J. Passeng. Cars - Mech. Syst.* 9(3):1047-1052, 2016, doi:10.4271/2016-01-1808.
8. Star-CCM+ User Guide (Version 11.06.010). CD-Adapco, 2017.
9. Nicoud, F. and Ducros, F., "Subgrid-Scale Stress Modelling Based on the Square of the Velocity Gradient Tensor," *Flow, Turbulence and Combustion* 62(3):183-200, 1999.
10. ANSYS 12.1, Help Manual. ANSYS, 2009.
11. Kaltenbacher, B., Kaltenbacher, M., and Sim, I., "A Modified and Stable Version of a Perfectly Matched Layer Technique for the 3-d Second Order Wave Equation in Time Domain with an Application to Aeroacoustics," *Journal of Computational Physics* 235:407-422, 2013.
12. Kaltenbacher, M., *Numerical Simulation of Mechatronic Sensors and Actuators: Finite Elements for Multiphysics* Third Edition (Springer, 2015).

Contact Information

Institute of Process Machinery and Systems Engineering, Friedrich-Alexander University of Erlangen-Nürnberg (FAU)
Cauerstrasse 4, 91058 Erlangen, Germany
tz@ipat.uni-erlangen.de
sb@ipat.uni-erlangen.de

Institute of Mechanics and Mechatronics, Vienna University of Technology
Getreidemarkt 9, 1060 Vienna, Austria
manfred.kaltenbacher@tuwien.ac.at

Acknowledgments

The authors would like to acknowledge the financial support of the *COMET - Competence Centers for Excellent Technologies Programme* of the Austrian Federal Ministry for Transport, Innovation and Technology (bmvit), the Austrian Federal Ministry of Science, Research and Economy (bmwfw), the Austrian Research Promotion Agency (FFG), the Province of Styria and the Styrian Business Promotion Agency (SFG).

ISSN 0148-7191